

Effective adsorption of phenols using nitrogen-containing porous activated carbon prepared from sunflower plates

Zhengguo Zhang*, Xiaoqin Feng*, Xiao-Xia Yue*, Fu-Qiang An*,†, Wen-Xia Zhou*,
Jian-Feng Gao*, Tuo-Ping Hu*,†, and Chin-Chuan Wei**

*Chemical Department, North University of China, Taiyuan 030051, P. R. China

**Biochemistry/Biophysics, Southern Illinois University Edwardsville, USA

(Received 13 March 2014 • accepted 9 December 2014)

Abstract—Nitrogen-containing porous carbons, the 800SP-NH₃, were synthesized using sunflower plates as the major carbon source carbonized at 800 °C and activated with concentrated aqueous ammonia at the same temperature. The porous carbons were characterized by nitrogen physical adsorption-desorption, surface area analyzer, FT-IR, and SEM. The adsorption properties of the porous carbons towards phenols were also investigated by batch methods. The test results show that the average pore diameter of porous carbon is smaller than 2 nm, and nitrogen-containing chemical groups are formed on its surface. The adsorption capacity for phenol, 4-chlorophenol, and p-nitrophenol is 316.5 mg/g, 330.24 mg/g and 387.62 mg/g due to its developed pore structure and nitrogen-containing chemical groups. The adsorption isotherm data greatly obey the Langmuir model.

Keywords: Porous Carbon, Nitrogen-containing, Adsorption, Phenols, Sunflower Plate

INTRODUCTION

Phenols, used widely in chemicals, pharmaceuticals, petroleum, coal gasification, papermaking, wood, rubber, dye and pesticide industries, are considered as priority organic pollutants by the US, China, and other countries due to their carcinogenic and highly toxic effects on organisms, unpleasant taste and odor even at low concentrations. In the US, according to the Environmental Protection Agency (EPA) regulations, the phenol content in the wastewater must be less than 1 mg/L [1]. In China, according to the Chinese integrated wastewater discharge standard (GB 8978-1996), the maximum permitted concentration of volatile phenols is 0.5 mg/L for standard A effluent and 2.0 mg/L for standard C effluent [2]. In Korea, the maximum permitted concentration of volatile phenols is 0.5 mg/L. Therefore, the effective removal of phenols from wastewater is very important and has attracted considerable research and practical interest.

Various methods, such as degradation [3-6], oxidation [7-9], solvent extraction [10,11], membrane separation [12-14], and adsorption [1,15-41], have been established and developed for removing phenols from wastewater. Among them, adsorption is an effective and widely used method to remove phenols from wastewater due to its higher capability and its relatively simple operability. Porous activated carbon has been deemed as one of the efficient adsorbents for removal of phenols from wastewaters because of its high surface area, well-developed internal pore structure and controllable surface functional groups. Biomass and polymers are the commonly used precursors to prepare porous carbons. Compared with

traditional non-renewable precursors, many agricultural wastes and industrial byproducts have been used as renewable precursors for activated carbon such as fruit shell, straw, peels, sewage sludge, fly ash, bagasse and so on [1,21-41].

In general, porous activated carbon is prepared at higher temperature and has few surface functional groups on its surface. So, the adsorption of porous carbon is mainly physical adsorption, and the adsorption capacity was poor. Besides the physical or porous structure, the surface functional groups are considered as the main influence factor of adsorption. To improve its adsorption property, surface chemical modification of porous carbon is desired. For example, nitrogen-containing chemical groups were incorporated after NH₃ or HNO₃ treating [42-44]. After chemical modification, its adsorption properties improved markedly.

In this work, nitrogen-containing porous carbons are synthesized using sunflower plates as raw material carbonized at 800 °C and activated with concentrated aqueous ammonia at 800 °C. The pore structure was determined, and the surface chemical groups of resultant porous carbon were characterized. Its adsorption properties for phenols were also investigated.

EXPERIMENTS

1. Materials and Instruments

Sunflower plates were obtained from a local farm in Shanxi Province, China. They were washed to remove mud and other impurities, dried at 105 °C for 24 h, subsequently crushed and sieved prior to the carbonization. Phenols and concentrated aqueous ammonia of analytical reagent were both purchased from Beijing chemical reagents factory, China.

Instruments used in this study were as follows: JWGB JW-BK132F surface area analyzer (Beijing, China), S-4800 field emission micro-

*To whom correspondence should be addressed.

E-mail: anfuqiang@nuc.edu.cn

Copyright by The Korean Institute of Chemical Engineers.

scope (Hitachi, Japan), FTIR4800S infrared spectrometer (Shimadzu, Japan), THZ-92C constant temperature shaker (Boxun Medical Treatment Equipment Factory of Shanghai, China), Unic-2602 UV spectrophotometer (Unic Company, American).

2. Synthesis of Porous Carbon

First, a certain amount of sunflower plate powder was carbonized in charcoal furnace at 800 °C for 2 h with heating rate of 3 °C/min with N₂ flow of 50 ml/min, and then activated in the same charcoal furnace using concentrated aqueous ammonia replacing the N₂. Finally, the resultant samples were washed with distilled water until neutral and dried at 80 °C for 24 h. The unactivated porous carbon, porous carbon activated with concentrated aqueous ammonia was denoted as 800SP and 800SP-NH₃, respectively.

3. Characterizations

The N₂ adsorption-desorption isotherms of 800SP and 800SP-NH₃ were obtained at 77 K using surface area analyzer. The samples were degassed under vacuum at 300 °C for 3 h prior to the measurement. The surface areas (S_{BET}) were estimated by Brunauer-Emmett-Teller (BET) method. The total pore volumes (V_{total}) were evaluated from the liquid volume of N₂ at a relative pressure (P/P₀) of 0.99. And the average pore diameters were from S_{BET} and V_{total} assuming an open-ended cylindrical pore model without pore networks. Micropore volume (V_{micropore}) was determined by Horvath-Kawazoe (HK) method, and mesopore volume (V_{mesopore}) was calculated by subtracting off V_{micropore} from V_{total}. The pore size distribution was determined by Barret-Joymer-Hanlenda (BJH) model.

The morphology of 800SP and 800SP-NH₃ was examined by scanning electron microscope. The samples were dried at 105 °C for 2 h and coated with a thin gold film to give electrical conduction on the carbon external surface. Fourier transform infrared (FT-IR) spectrum of the sample was measured on FTIR4800S spectrometer using the usual KBr pellet technique (Shimadzu, Japan).

4. Adsorption Experiments

Batch equilibrium adsorption experiments were performed using about 0.01 g of adsorbent and 50 mL of phenols solution. After adsorption reached equilibrium, the adsorbent separated from the samples by filtering and the filtrate was analyzed with a UV spectrophotometer. The influences of contact time and initial phenols concentration were studied by batch method. The adsorption capacity (Q_e) was calculated according to the following equation:

$$Q_e = [(C_0 - C_e)/m] \times V$$

where, C₀ and C_e is the initial and equilibrium concentration of phenols in the solution (mg/L), V is the volume of the solution (L), and m is the dosage of adsorbent (g).

RESULT AND DISCUSSION

1. Characterization of Porous Carbon Structure

The N₂ adsorption-desorption isotherms of the 800SP and 800SP-NH₃ at 77 K are shown in Fig. 1.

It is clear that the shape of N₂ adsorption-desorption isotherm changes after being activated with concentrated aqueous ammonia. 800SP gives type I and II with a hysteresis loop of type H₂. This indicates that 800SP has a great quantity of mesopores, while 800SP-NH₃ gives a steep type I isotherm with a small hysteresis loop of

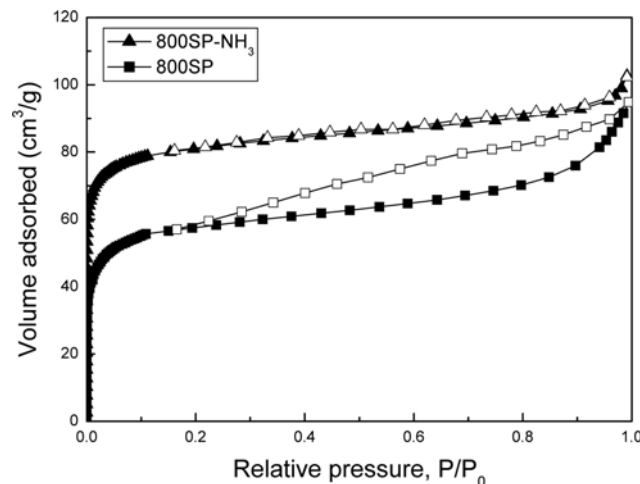


Fig. 1. N₂ adsorption-desorption isotherms.

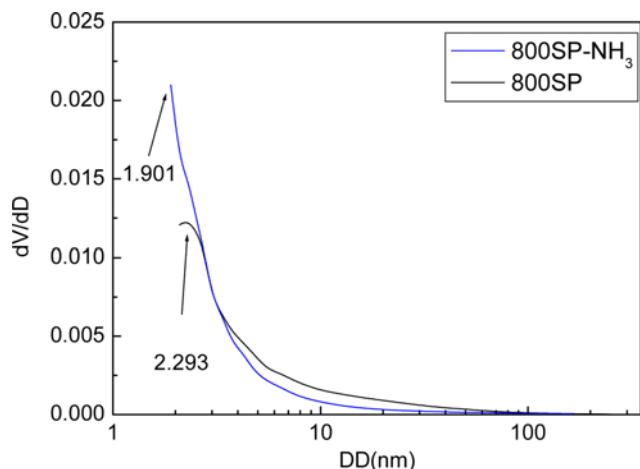


Fig. 2. Pore size distributions of porous carbons.

type H₄. The adsorption of N₂ increases rapidly at low relative pressure (P/P₀<0.10) and then approaches a plateau with increasing the relative pressure. The adsorption and desorption curves were almost overlapped, which indicates that a large amount of micropores with a highly narrow pore size distribution were developed.

The pore size distributions and most probable pore size of samples are shown in Fig. 2. The pore properties of the 800SP and 800SP-NH₃ are listed in Table 1.

The pore size distribution is narrow, the average pores size of 800SP-NH₃ was 1.942 nm, and the V_{micropore} of 800SP-NH₃ accounted for 75.40% of V_{total}. These indicate again that there is a large number of micropores in 800SP-NH₃. It can also be seen that the BET special surface area and pore volume is increased after activation

Table 1. The pore structure parameters

Samples	S _{BET} (m ² /g)	V _{total} (cm ³ /g)	V _{micropore} (cm ³ /g)	V _{mesopore} (cm ³ /g)	Pore size (nm)
800SP	221.09	0.147	0.075	0.072	2.655
800SP-NH ₃	385.26	0.289	0.218	0.071	1.942

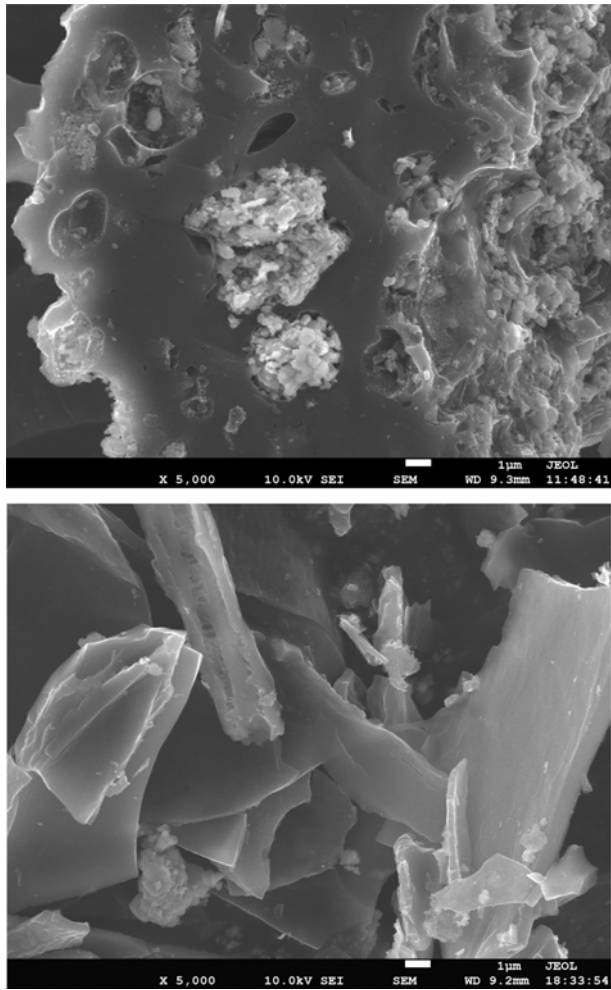


Fig. 3. SEM images of porous carbons. (a) 800SP, (b) 800SP-NH₃.

with concentrated aqueous ammonia. The increase of BET specific surface area and pore volume indicated that the number of pores increased.

The SEM images of porous carbons are shown in Fig. 3.

The surface of the 800SP is relatively coarse as some carbon particles fill the big pores and are attached to the surrounding surface. When the 800SP is activated, the surface becomes smooth, because the filled and attached carbon particles are removed. So, the BET specific surface area and pore volume increases. This is consistent with the former structure analysis.

The presence of the nitrogen-containing groups in the prepared porous carbons is confirmed by FT-IR spectroscopy (Fig. 4).

In the spectra of 800SP-NH₃, new adsorption bands appeared at 711 and 1,618 cm⁻¹. These are assigned to the characteristic absorption of N-H. This evidenced the introduction of amine in the surface of activated carbon.

2. Adsorption Properties of Porous Carbon Towards Phenols

The kinetic adsorption curve of the 800SP and 800SP-NH₃ towards phenols is shown in Fig. 5.

The saturated adsorption capacity of the 800SP and 800SP-NH₃ towards phenol is 128.9 mg/g and 316.5 mg/g, respectively. The adsorption capacity of 800SP-NH₃ is higher than that of 800SP. This

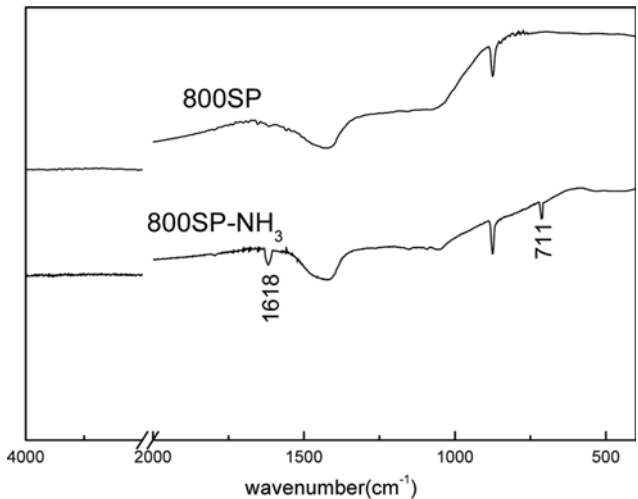


Fig. 4. FT-IR spectra.

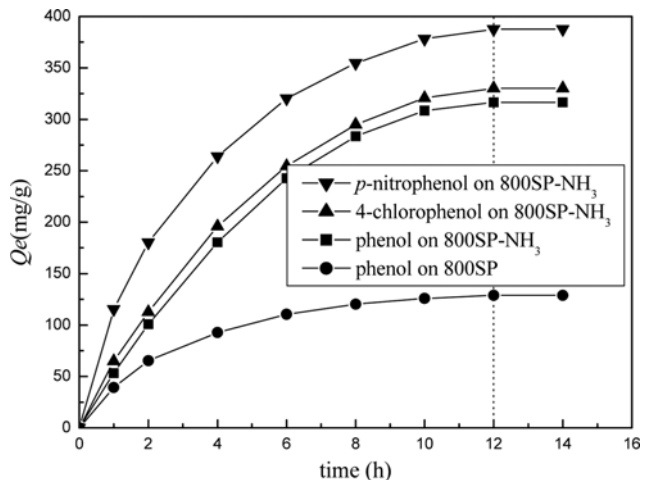


Fig. 5. Adsorption kinetic curves of 800SP and 800SP-NH₃ for phenols. Temperature: 20 °C; pH 6.

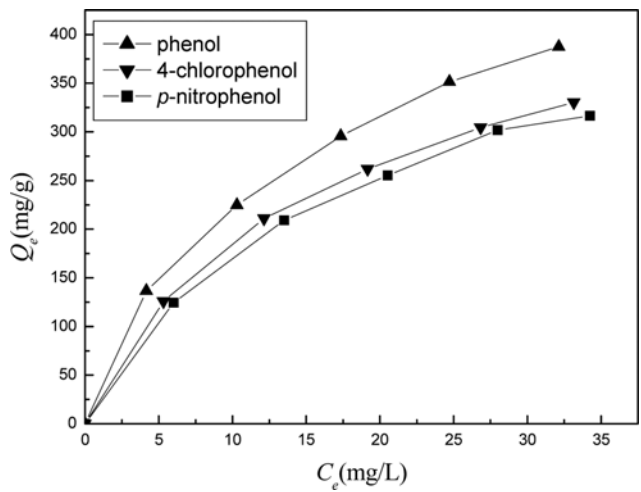


Fig. 6. Adsorption isotherms of 800SP-NH₃ towards phenol. Temperature: 20 °C; Time: 12 h; pH 6.

Table 2. Comparisons of adsorption capacity (mg/g) towards phenols by other AC adsorbents

Precursors of AC adsorbents	Adsorbate	Adsorption capacity	Reference
Sunflower plates	Phenol	316.5	This study
Sunflower plates	4-Chlorophenol	330.24	This study
Sunflower plates	p-Nitrophenol	387.62	This study
Cherry stone	Phenol	85	[1]
Corn grain	Phenol	190	[21]
Date-pit	Phenol	70	[22]
Avocado kernel seeds	Phenol	85	[23]
Hydrothermal char	Phenol	75	[24]
Sewage sludge	Phenol	190	[25]
Sewage sludge	4-Chlorophenol	320	[25]
Brown seaweed	Phenol	15	[26]
Tabacco residues	Phenol	12	[27]
Oil palm empty fruit bunch	2,4-Dichlorophenol	250	[28]
Almond shell	Phenol	125	[29]
Almond shell	p-Nitrophenol	210	[29]
Vine shoots	Phenol	75	[29]
Vine shoots	p-Nitrophenol	220	[29]
Pokeweed	Phenol	170	[30]
Vinegar lees	Phenol	120	[31]
Bagasse fly ash	Phenol	3.22	[32]
Coffee grounds	p-Nitrophenol	100	[33]
Melon seeds	p-Nitrophenol	97	[33]
Orange peels	p-Nitrophenol	100	[33]
Sewage sludge	Phenol	176	[34]
Sugarcane bagasse	Phenol	25	[35]
Soybean straw	Phenol	278	[36]
Albizia lebbeck seed pods	4-Chlorophenol	247.9	[37]
Coconut shell	Phenol	60	[38]
Olive stone	Phenol	27	[39]
Switch grass	Phenol	94	[40]
Eggshells	Phenol	180	[41]
Lignite activated carbon	Phenol	230	[45]
S.D. Fine Chemicals Boisar, India	Phenol	140	[46]
CPG-LF	Phenol	80	[47]
MN-200	Phenol	50	[47]
XAD-2	Phenol	70	[47]

is attributed to the developed pore structure, high specific surface and the surface modification with the functional groups in the 800SP-NH₃ structures.

Additionally, the 800SP-NH₃ prepared in this study possesses higher adsorption capacity for other phenols than previously reported porous carbons including some commercialized activated carbons, and the comparisons are shown in Table 2. This illustrates that 800SP-NH₃ possesses very strong adsorption ability and high affinity for phenols, and they can be used to remove effectively phenols.

The adsorption isotherm of 800SP-NH₃ towards phenol is shown in Fig. 6.

To investigate the equilibrium adsorption behavior of phenol on porous carbon, it was important to have a satisfactory description of the quantitative relationship between the two phases in the ad-

sorption system. The adsorption isotherm is fitted by the Langmuir model [48,49].

$$\text{Langmuir isotherm: } C_e/Q_e = C_e/Q_0 + 1/(KQ_0)$$

where C_e (mg/L) was the equilibrium concentration, Q_e (mg/g) was the equilibrium adsorption capacity, Q₀ (mg/g) was the monolayer sorption capacity, K (L/mg) was the Langmuir constant related to the adsorption energy.

The linear regression equations, parameters and the correlation coefficient are listed in Table 3.

From the values of R² in Table 3, it can be concluded that the Langmuir equations fit best to the experimental data. Thus, the applicability of monolayer coverage of phenol on the surface of the activated carbon is confirmed.

Table 3. Adsorption linear regression equations of 800SP-NH₃ towards phenol

Adsorption model	Langmuir
Linear regression equation	$C_e/Q_e = 0.002C_e + 0.0378$
R ²	0.9954
K	0.053
Q ₀	500

CONCLUSION

Nitrogen-containing porous carbon with high surface area and large pore volume was synthesized successfully from sunflower plates carbonized at 800 °C and activated with concentrated aqueous ammonia at the same temperature. The BET specific surface area is as high as 311.79 m²/g. The microporous structure and presence of nitrogen-containing groups was confirmed. The nitrogen-containing microporous carbon displayed fast and high adsorption capacities for phenols due to its developed pore structure and nitrogen-containing chemical groups, the adsorption capacities towards phenol, 4-chlorophenol, and *p*-nitrophenol were 316.5 mg/g, 330.24 mg/g and 387.62 mg/g, respectively. The adsorption isotherm data greatly obey the Langmuir model.

ACKNOWLEDGEMENTS

The authors gratefully acknowledge the financial support of this work by the International Science & Technology Cooperation Program of China (No. 2011DFA51980), Shanxi Science & Technology Cooperation Program of China (No. 2011DFA51980), National Scientific Foundation of China (No. 5110423), and Science Foundation of Shanxi Province (No. 20130321022-02, 2013021012-3, 20140313002-4).

REFERENCES

- U. Beker, B. Ganbold, H. Dertli and D. D. Gülbayır, *Energy Convers. Manage.*, **51**, 235 (2010).
- J. Yin, R. Chen, Y. Ji, C. Zhao, G. Zhao and H. Zhang, *Chem. Eng. J.*, **157**, 466 (2010).
- S. Yu, H. J. Yun, Y. H. Kim and J. Yi, *Appl. Catal. B-Environ.*, **144**, 893 (2014).
- F. Zaviska, P. Drogui, E. M. E. Hachemi and E. Naffrechoux, *Ultrasound. Sonochem.*, **21**, 69 (2014).
- G. Hurwitz, P. Pornwongthong, S. Mahendra and E. M. V. Hoek, *Chem. Eng. J.*, **240**, 235 (2014).
- E. M. Seftel, M. C. Puscasu, M. Mertens, P. Cool and G. Carja, *Appl. Catal. B-Environ.*, **150-151**, 157 (2014).
- W. M. Wang, J. Song and X. Han, *J. Hazard. Mater.*, **262**, 412 (2013).
- R. Carta and F. Desogus, *J. Environ. Chem. Eng.*, **1**, 1292 (2013).
- A. B. Ayusheev, O. P. Taran, I. A. Seryak, O. Y. Podyacheva, C. Descorme, M. Besson, L. S. Kibis, A. I. Boronin, A. I. Romanenko, Z. R. Ismagilov and V. Parmon, *Appl. Catal. B-Environ.*, **146**, 177 (2014).
- C. Zidi, R. Tayeb and M. Dhahbi, *J. Hazard. Mater.*, **194**, 62 (2011).
- N. N. M. Zain, N. K. A. Bakar, S. Mohamad and N. M. Saleh, *Spec. trochim. Acta A*, **118**, 1121 (2014).
- S. Shen, S. E. Kentish and G. W. Stevens, *Sep. Purif. Technol.*, **95**, 80 (2012).
- A. Hasanoğlu, *Desalination*, **309**, 171 (2013).
- P. Praveen and K. C. Loh, *J. Membr. Sci.*, **437**, 1 (2013).
- S. S. Mehdi, S. J. Jafari, M. Farrokhi and J. K. Yang, *Environ. Eng. Res.*, **18**, 247 (2013).
- S. Larous and A. H. Meniai, *Energy Procedia*, **18**, 905 (2012).
- F. Belaib, A. H. Meniai and M. B. Lehocine, *Energy Procedia*, **18**, 1254 (2012).
- A. Gładysz-Płaska, M. Majdan, S. Pikus and D. Sternik, *Chem. Eng. J.*, **179**, 140 (2012).
- G. Qin, Y. Yao, W. Wei and T. Zhang, *Appl. Surf. Sci.*, **280**, 806 (2013).
- C. Păcurariu, G. Mihoc, A. Popa, S. G. Muntean and R. Ianoş, *Chem. Eng. J.*, **222**, 218 (2013).
- K. H. Park, M. S. Balathanigaimani, W. G. Shim, J. W. Lee and H. Moon, *Micropor. Mesopor. Mater.*, **127**, 1 (2010).
- M. H. El-Naas, S. Al-Zuhair and M. A. Alhaija, *Chem. Eng. J.*, **162**, 997 (2010).
- L. A. Rodrigues, M. L. C. P. da Silva, M. O. Alvarez-Mendes, A. R. Coutinho and G. P. Thim, *Chem. Eng. J.*, **174**, 49 (2011).
- Z. G. Liu and F. S. Zhang, *Desalination*, **267**, 101 (2011).
- V. M. Monsalvo, A. F. Mohedano and J. J. Rodriguez, *Desalination*, **277**, 377 (2011).
- A. Rathinam, J. R. Rao and B. U. Nair, *J. Taiwan Inst. Chem. Eng.*, **42**, 952 (2011).
- M. Kilic, E. Apaydin-Varol and A. E. Pütün, *J. Hazard. Mater.*, **189**, 397 (2011).
- F. W. Shaarani and B. H. Hameed, *Chem. Eng. J.*, **169**, 180 (2011).
- P. A. M. Mourão, C. Laginhas, F. Custódio, J. M. V. Nabais, P. J. M. Carrott and M. M. L. Ribeiro Carrott, *Fuel Process. Technol.*, **92**, 241 (2011).
- Y. D. Chen, M. J. Huang, B. Huang and X. R. Chen, *J. Anal. Appl. Pyrol.*, **98**, 159 (2011).
- M. Zhong, Y. Wang, J. Yu, Y. Tian and G. Xu, *Particuology*, **10**, 35 (2012).
- C. W. Purnomo, C. Salim and H. Hinode, *Fuel Process. Technol.*, **102**, 132 (2012).
- D. Djilani, R. Zaghdoudi, A. Modarressi, M. Rogalski, F. Djazi and A. Lallam, *Chem. Eng. J.*, **189-190**, 203 (2012).
- D. Li, Y. Wu, L. Feng and L. Zhang, *Bioresour. Technol.*, **113**, 121 (2012).
- H. D. S. S. Karunaratne and B. M. W. P. K. Amarasinghe, *Energy Procedia*, **34**, 83 (2013).
- Q. Miao, Y. Tang, J. Xu, X. Liu, L. Xiao and Q. Chen, *J. Taiwan Inst. Chem. Eng.*, **44**, 458 (2013).
- M. J. Ahmed and S. K. Theydan, *J. Anal. Appl. Pyrol.*, **100**, 253 (2013).
- S. J. Kulkarni, R. W. Tapre, S. V. Patil and M. B. Sawarkar, *Procedia Eng.*, **51**, 300 (2013).
- N. Soudani, S. Souissi-najar and A. Ouederni, *Chinese J. Chem. Eng.*, **21**, 1425 (2013).
- Y. Han, A. A. Boateng, P. X. Qi, I. M. Lima and J. Chang, *J. Environ. Manage.*, **118**, 196 (2013).
- L. Giraldo and J. C. Moreno-Piraján, *J. Anal. Appl. Pyrol.* (2014),

- [http://dx.doi.org/10.1016/j.jaap.2013.12.007.](http://dx.doi.org/10.1016/j.jaap.2013.12.007)
42. Y. S. Yun, D. Kim, H. H. Park, Y. Tak and H. Jin, *Synth. Met.*, **162**, 2337 (2012).
43. R. Pietrzak, *Fuel*, **88**, 1871 (2009).
44. M. H. Kasnejad, A. Esfandiari, T. Kagnazchi and N. Asasian, *J. Taiwan Inst. Chem. Eng.*, **43**, 736 (2012).
45. G. C. Lv, J. Hao, L. Liu, H. W. Ma, Q. F. Fang, L. M. Wu, M. Q. Wei and Y. H. Zhang, *Chinese Chem. Eng.*, **19**, 380 (2011).
46. S. Kumar, M. Zafar, J. K. Prajapati, S. Kumar and S. Kannepalli, *J. Hazard. Mater.*, **185**, 287 (2011).
47. U. Beker, B. Ganbold, H. Dertli and D. D. Gulbayir, *Energy Convers. Manage.*, **51**, 235 (2010).
48. C. X. Zhang, Q. Q. Qiao, J. D. A. Piper and B. C. Huang, *Environ. Pollut.*, **159**, 3057 (2011).
49. S. Hena, *J. Hazard. Mater.*, **181**, 474 (2010).